heritage

MDPI

Article

Mass-Transfer Air Pollution Modeling in Heritage Buildings

Morten Ryhl-Svendsen * and Signe Hjerrild Smedemark †

Institute for Conservation, Royal Danish Academy, 1435 Copenhagen, Denmark; signe.hjerrild.smedemark@hum.ku.dk

* Correspondence: mrsv@kglakademi.dk; Tel.: +45-4170-1929

† Current address: Department of Nordic Studies, and Linguistics, University of Copenhagen, 2300 Copenhagen, Denmark.

Abstract: Two simple mass-balance models for estimating the concentration of air pollutants inside buildings are presented for pollutants originating from outdoors or generated indoors. The models can be used to establish average pollution loads on heritage objects inside buildings and assist in risk assessment for conservation. The models can be run with a minimum of data, either based on fixed conditions or as a Monte Carlo simulation based on plausible intervals of the input factors. Input data can be obtained by simple measurements or based on the literature. A museum storage hall in Denmark was used as a test site for demonstrating the models. They were evaluated with regard to the prediction of the indoor/outdoor concentration ratio for ozone and nitrogen dioxide and the build-up concentration of indoor generated organic acids. The pros and cons of such models were discussed, where the main reservation is related to shortcomings when real buildings are more complicated than the single-zone structure of the models. A strength of the models is the easy adaption to an indoor environment and, despite being semi-quantitative at times, the simplicity of the models, which allows for practical everyday use in air quality management of heritage buildings.

Keywords: mass-balance; emission; deposition velocity; ozone; nitrogen dioxide; organic acids; indoor-outdoor ratio; indoor air pollution; Monte Carlo simulation

Citation: Ryhl-Svendsen, M.; Smedemark, S.H. Mass-Transfer Air Pollution Modeling in Heritage Buildings. *Heritage* **2023**, *6*, 4768–4786. https://doi.org/10.3390/heritage6060253

Academic Editors: Peter Brimblecombe and Jenny Richards

Received: 15 May 2023
Revised: 9 June 2023
Accepted: 10 June 2023
Published: 12 June 2023

1. Introduction

Air pollution is recognized to cause damage to a wide range of heritage materials, e.g., by direct oxidation or by conversion into acid at contact [1–3]. Pollutants may be present in outdoor air or have local, indoor sources. The main gaseous outdoor pollutants known to cause damage to heritage collections are ozone, nitrogen dioxide, and various sulfur compounds, and may have both natural and anthropogenic sources [4–6]. The most critical indoor air pollutants known to engage in material damage are formic acid and acetic acid (in this paper, "organic acids" is used to refer to formic acid and acetic acid collectively) [4–7]. Wood, a common heritage material, as well as a widely used construction material, is known to emit organic acids and is one of the main indoor sources of this type of compound in indoor air [8–10].

Outdoor pollutants will, other things being equal, become reduced to a fraction of the outdoor level when the compounds infiltrate a building, either directly through forced ventilation systems, open windows, etc., or by natural ventilation at tortuous paths bypassing closed but leaky doors, or through small leaks, cracks, and holes in the building envelope. If, on the other hand, indoor pollution sources are present, the indoor level can exceed the outdoor level by many orders of magnitude [11]. Several publications collate typical pollution levels in museums and other heritage buildings [6,12–15], and guidelines on pollution levels for the preservation of heritage objects are given, for example, by the American Society of Heating, Refrigerating and Air-Conditioning Engineers (ASHRAE) [16].

In order to assess the risk associated with air pollution for a heritage collection, the pollution levels must be known. This can be obtained either by measurement or by calculation based on other available data. Even though air pollution monitoring solutions

are becoming increasingly cheap and available [17], air quality monitoring for a range of pollutants, and maybe in several locations at one time, is often more comprehensive than what most museums have the resources for. Instead, air pollution models are a useful and cost-effective mean to evaluate conservation conditions for heritage buildings without having to initiate large and expensive monitoring campaigns. Model input can be based on easily accessed outdoor pollution data from public air pollution monitoring network and for indoor-generated compounds by data from the literature on material's emissions.

As will be described below, models for indoor air pollution are available in many levels of complexity. However, while advanced models are suitable for detailed research and for gaining a fundamental understanding of air quality mechanisms, they may not be feasible for everyday long-term surveying. In that case, a sufficient and useful estimate of the pollution load in a heritage building can be obtained by more simple mathematical expressions based on basic yet decisive factors. Besides being easy to use and understand, the output provides sufficient information necessary for assessing the risk of material damage. As damage to heritage objects caused by air pollutants depends on the dose rather than its momentary concentration in the air [6,18,19], steady-state calculations, rather than modeling dynamic situations, are fully comprehensive for predicting conservation conditions in heritage environments.

In this paper, we demonstrate such models, which provide an effective and easy estimation of gaseous air pollution levels to be used in practice for conservation risk assessment in buildings containing heritage collections. Table 1 lists the nomenclature used throughout the paper.

Table 1. Nomenclature used in this paper: Symbols and their units.

Symbol	Description	Unit
A	Surface area	m^2
C_i	Indoor concentration of a pollutant in the air	$\mu g\ m^{-3}$
C_o	Outdoor concentration of a pollutant in the air	$\mu g\ m^{-3}$
I/O	Ratio between indoor and outdoor pollution concentration	Dimensionless
L	Loading: The surface-to-volume ratio of objects or materials in a room. $L = A/V$	$m^2\ m^{-3}$
n	Air exchange rate (exchange of air with ambient)	$hour^{-1}$
Q	Air flow rate (e.g., through a filter unit)	$hour^{-1}$
S	Surface removal rate. $S = v_d(A/V)$	$hour^{-1}$
SER	Area-specific emission rate of a pollutant from a material	$\mu g\ m^{-2}\ h^{-1}$
V	Room volume	m^3
v_d	Deposition velocity of a pollutant in the air onto a surface	$m\ hour^{-1}$

2. Indoor Air Pollution Models

In its most basic form, the level of outdoor pollutants can be approximated for indoor environments by the "100/10/1" rule-of-thumb by Tetreault [6] (pp. 35–38). It suggests, as a generalization, that outdoor pollutants will be decimated from a 100% presence outdoors to about 10% inside a building and again down to about 1% of the outdoor level inside smaller indoor enclosures such as display cases, cabinets, etc. As simple as it may sound, the "100/10/1" rule provides a fair idea of which order of magnitude one may expect for air pollution inside a museum building if the outdoor pollution level is known. The ratio between the three locations, outdoors, room, and confined enclosure, reflects a mass-balance based on several factors (building geometry and characteristics, weather, use of the building, etc.), which control the transfer of air between the different zones.

2.1. Mass-Balance at Steady-State

Mass-balance models are based on the fundamental principle of mass conservation and can be expressed as an ordinary differential equation that balances sources and sinks [20,21] (pp. 57–65):

$$\frac{dC_i}{dt} = C_{Sources} - C_{Sinks} \quad (1)$$

where C_i is the concentration at steady-state, t is time, $C_{sources}$ the influx, and C_{sinks} is the loss.

Such expressions are fast to compute and can provide a basic means to model air pollution in buildings or rooms that can be treated as a single zone, e.g., one room surrounded by ambient environment, and assumes well-mixed air (uniform distribution of pollutants throughout a zone). The mass-balance calculates the concentration at steady-state conditions.

2.2. Indoor-Outdoor Ratio (I/O)

Weschler et al. [22] presented a steady-state mass-balance model to determine the ozone concentration that one can expect inside a building if the outdoor level is known. This relation is also known as the I/O (indoor/outdoor) ratio. Several parameters must be known to use the I/O model. It treats the building (or room) as a single zone and uses the outdoor concentration together with the air change rate (n), the deposition velocity of the pollutant onto an internal surface (v_d), the ratio between the surface area of materials in the zone and the volume of the zone (A/V), in order to estimate the concentration of ozone indoors:

$$\frac{C_i}{C_o} = \frac{n}{n + \left(v_d \times \frac{A}{V}\right)} \quad (2)$$

The surface-to-volume ratio (A/V) is also called the loading of material (L). The deposition velocity expresses the rate at which the pollutants react on surfaces. It is defined as the flux of the pollutant toward a surface divided by its concentration in the air and is by this a mass-transfer coefficient with the unit of velocity [23]. The factor $v_d(A/L)$ from Equation (2) expresses the loss of pollutants by surface uptake (sorption reactions). This is often referred to as the surface removal rate (S) [24], and is comparable to an air exchange rate with which it shares unity (number of room volumes removed per unit time). For a room with several materials present ($material_1$, $material_2$, $material_3$, ...), the total surface removal rate S is the sum of each material's surface removal rate (S_1, S_2, S_3, ...):

$$\frac{C_i}{C_o} = \frac{n}{n + (S_1 + S_2 + S_3 + \ldots)} \quad (3)$$

The I/O model was put forward only for ozone [22], but since then, it has been used for other pollutants as well, such as nitrogen dioxide and sulfur dioxide [25]. The model assumes that the air pollutants are removed only through deposition onto surfaces or by ventilation. According to Spicer et al. [26], this is a reasonable assumption for reactive gaseous outdoor air pollutants, although pollutants, such as nitrogen dioxide, are known to engage in heterogeneous reactions and be re-released as nitrous and nitric acid [27,28]. Reactions in the air are also disregarded, although, for example, the production of nitrogen dioxide by atmospheric reactions involving ozone and nitrogen oxide may take place indoors [29].

In heritage studies, the I/O model has been known as the "IMPACT model" due to its use in an online I/O calculator aimed for museums and other heritage buildings, developed through the European research project "Innovative Modelling of Museum Pollutants and Conservation Thresholds" (IMPACT) [25]. The online IMPACT calculator is currently not available. However, the I/O model (Equation (2)) can easily be set up in Microsoft Excel or similar spreadsheet software. Deposition velocities are available in the literature for a range of pollutants and materials, for example [30].

2.3. Indoor Air Pollution (IAP)

A steady-state balance similar to that of Equations (2) and (3) can be expressed for pollutants generated within the indoor zone (the building, the room) [31,32]:

$$C_i = \frac{SER \times L}{n + S} \quad (4)$$

The IAP model assumes the outdoor concentration $C_o = 0$ and treats the building as a single zone. The indoor generation of pollutants happens as emission from materials, and in the case of museum environments, especially the release of organic acids is considered harmful for a range of heritage materials [4–6]. The area-specific emission rate *SER* of organic acids has been measured for samples of heritage wood objects [10], and the IAP model has previously been applied to museum storage environments [31,32]. Smedemark and Ryhl-Svendsen [32] provided a general step-by-step guide to its use based on easily measured building characteristics and data collated from the literature. This approach is used in the present study as well (see Section 4 below).

2.4. Monte Carlo Simulations

The factors which the air pollution models depend on may be difficult to estimate precisely. Some parameters may vary widely between sites or within the same building over time. It can, therefore, be difficult to choose one specific value for each factor without giving rise to a large uncertainty in the calculated pollution level. Instead, it may be desirable to model within a given interval (for example, expected variation in the air exchange rate or uncertain estimation of surface areas of objects). In the case of the I/O ratio and IAP models, some parameters remain constant and are easy to measure (e.g., room volume), while others may vary within a given interval, influenced continuously by climate or by sudden impacts caused by human activity (Figure 1).

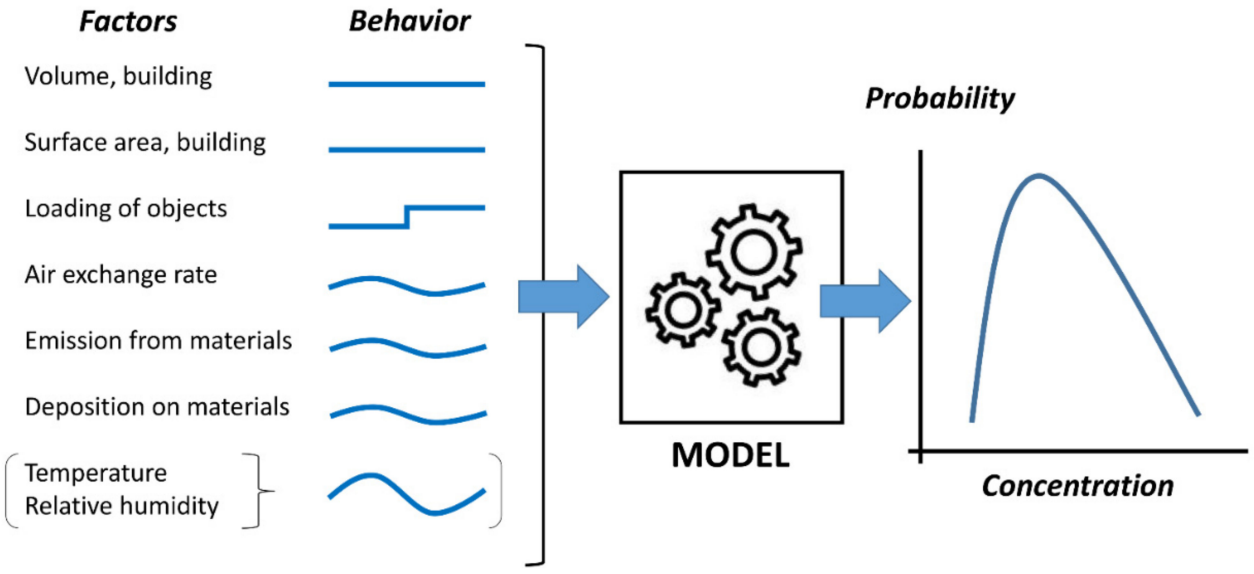

Figure 1. Principal sketch of factors influencing air pollution modeling and their possible behavior. Some factors remain constant over time (straight line), some may change due to sudden events (jagged line) or by more or less continuous variations (curved lines). Temperature and humidity are not directly included in the models. However, indirectly, they influence other factors such as emission rate. Together they result in a range of more or less probable outputs (concentrations).

A Monte Carlo simulation is a statistical tool that can be used to model an output that depends on several random variables. The parameters are defined as an interval, and a probability distribution is assigned to each variable. The results are obtained through

repeated random sampling over numerous model runs. Monte Carlo simulations have previously been used in several indoor air pollution studies [32–36].

2.5. Other Computational Simulations

It must be stressed that the simple models of Equations (2)–(4) do not take into account all the variables which affect indoor air pollution levels. Chemical reactions may take place in the air or on surfaces, which re-release new compounds [37,38]. This is especially relevant for nitrogen oxides [27,28]. While detailed chemical models exist [39,40], they are much more complex than what is necessary for day-to-day air quality assessment for heritage buildings and will not be dealt with here. Although such models have indeed been applied to heritage environments, this has mainly been for short-term continuous monitoring periods with a focus on time-resolved measurements [41–43].

A number of non-constant factors influence emission and deposition rates, e.g., temperature and relative humidity [10,30]. Air exchange may vary, and the air movement and turbulence in a room create variations and gradients in the indoor environments, which are not reflected in the simple steady-state models as they assume a perfect mixing of air within a space. Instead, fluid simulations (computational fluid dynamics, CFD) can be used to explore such situations [44]. Again, although the use of CFD indeed has a place also for heritage environment research, it requires expert know-how to use and may primarily be applied for exploring special situations where airflow within a room must be visualized [45], or as an integrated part of designing buildings together with climate and energy consumption simulations [46].

Particle pollution loads can be described by expressions similar to those of the gaseous compound models, e.g., I/O ratio [47,48]. However, other, more specific mechanisms do also influence particle infiltration and deposition (among other things, particle size, aerodynamic properties, gravity, and thermophoresis-related phenomena) [49–51]. These conditions cannot be given the attention they deserve within the limits of this paper. Therefore, particle modeling will not be dealt with.

3. Case Study

3.1. The National Museum Storage Facility

For the demonstration of the application of mass-balance models, we take as an example a newly built Danish storage facility. Located in the town Vinge, about 40 km outside Copenhagen, the building contains the largest heritage storage facility in Northern Europe. The facility, designed by Gottlieb Paludan Architects and MOE Consulting Engineers, opened in May 2022, and will house the main part of the collections of The National Museum of Denmark and the Danish Royal Library [52].

The entire facility has about 25,000 m^2, which, besides storage areas, includes an indoor truck bay, service areas, pest disinfection chambers, workshops, and offices. The library part of the storage facility is mechanically cooled for the keeping of chemically unstable collections (e.g., acid paper), while the main hall for museum objects is without active temperature control. This part of the storage area is designed following the low-energy concept previously developed and put in use in several Danish storage buildings [53,54]. We focus here on the National Museum's part of the facility, which is the main, unheated storage hall (Figures 2 and 3).

3.2. The Building

The storage building has a well-sealed building envelope with a low air change rate. The exact air exchange rate is not known (not yet measured) but assumed to be on the order of 0.5 per day (0.02 h^{-1}). There are no windows, and entrances are fitted with double-door airlocks in order to reduce the impact of the outdoor climate.

The storage hall contains eight adjacent storage sections, separated by rolling gates (Figure 2). Each section measures 1000 m^2 with a volume of 9400 m^3 (total 8000 m^2 and 75,200 m^3). Despite the division in eight sections (due to fire sectioning), the eight closely

connected areas can be regarded as one large, combined storage volume, which shares the internal distribution of air, and by this, a uniform climate and air quality.

Figure 2. A view down the central aisle that connects the storage sections, of the still empty storage hall. Photo by the authors.

Figure 3. A compact-shelves section, about half-full, with wooden furniture. Photo by the authors.

A ventilation system is in place for humidity control by mechanical dehumidifiers (desiccant type). It runs entirely by internal recirculation and without intake of ambient air.

The relative humidity is maintained at a moderate level (set-point 50% RH, limits 40–60% RH). The ventilation loop is only running when dehumidification is needed, and is VAV (variable air volume) controlled, with a maximum recirculation rate of 0.3 room volume per hour. The recirculated air passes through a combined particle and chemical air filter (Camfil City-Flo combination bag filter, particle filter grade F7 with broad-spectrum carbon media; Camfil, Stockholm, Sweden, https://www.camfil.com/ (accessed on 1 May 2023)). The hall is unheated and has been designed to always remain below 20 °C, however, the actual thermal performance has still to be validated by a full year of normal operation.

3.3. Ambient Conditions

The facility is located in a rural area near the small city of Frederikssund, and a few km from Roskilde Fjord. Danish climate is within a temperate climate zone (Köppen classification Dfb), and the ambient pollution level of the area is about 60 μg m^{-3} ozone and 6 μg m^{-3} nitrogen dioxide annual average (data from the national air pollution monitoring program at station Risø, 15 km away) [55].

3.4. Collection and Interior

Work started in 2022 to move in collection objects, however, this operation will take years due to derivative tasks, such as cleaning, pest disinfection procedures, and documentation along the moving process. At the time of writing (Spring 2023), the facility is loosely estimated 20% full. The collection contains a large variety of cultural history objects of many types of materials (wood, metals, painted objects, plastics, etc.). However, the vast majority are wooden objects. For simplicity in the present modeling study, we regard the collection items to be a uniform quantity of wooden objects (e.g., furniture, see Figure 3).

The storage is equipped with mobile compact shelves, which allow for storing objects at a high storage capacity (Figure 3). The shelves are made of powder-coated and galvanized steel. Other main materials present in the storage areas are concrete (walls and ceiling) and epoxy paint (floor). In Table 2, the surface area and loading (ratio of surface area to room volume) are given for each class of materials.

Table 2. Distribution of materials in one section of the storage hall. Materials are assumed to be equally distributed in all eight sections.

Material	Area [m^2]	Loading [m^2 m^{-3}]
Wall and ceiling (concrete)	4300	0.5
Floor (syntetic paint)	1000	0.1
Shelves (metal)	1000	0.1
Objects (wood), now	6500	0.7
Objects (wood), when full	28,000	3.0

4. Methods

The performance of the storage hall with regard to indoor air quality was demonstrated first for outdoor pollutants by the I/O model, followed by a prediction of indoor air pollution levels by the IAP model. Both models predict the pollution levels at steady-state conditions, however, we demonstrate how the steady state will vary at different air exchange rates. The IAP model was then used as the basis for a series of Monte Carlo simulations taking possible variations of the input parameters into account.

Several of the parameter values were estimates. The air exchange rate of the storage hall has not yet been validated by measurement. However, based on previous measurements, probable values were assumed [13]. Data on heritage materials' emission rates, as well as deposition rates for organic acids, are scarce. The input values, many of which are assumptions, were mainly taken from previous model studies [31,32]. Deposition velocity data for ozone and nitrogen dioxide were given by Grøntoft and Raychaudhuri [30].

The dimensions of the storage area, its interior, ventilation system, and the loading and nature of objects, were measured and observed at visits onsite, and by consulting

architectural drawings and technical descriptions of the building. The estimation of objects' loading is subject to some uncertainty, as the museum objects are all different in size and complex in shape (object types include furniture, household utensils, musical instruments, wooden sculptures, timber objects for buildings, etc.). For one typical shelf section, we measured the projected surface area of all objects in great detail. From this, we calculated the average object surface-area per running meter shelf, which was then multiplied up to the full storage capacity.

4.1. I/O Model

The I/O ratio was calculated by Equation (2) for the storage hall when full, assuming an air exchange rate of 0.02 h^{-1}, loading of materials as given in Table 2, and for each material the deposition velocities given in Table 3. From this, I/O ratios and the distribution of the pollution loss on the different material surfaces were calculated for ozone and nitrogen dioxide. For ozone and nitrogen dioxide, it was modeled how the I/O depends on the air exchange rate. Calculations were performed in Microsoft Excel using Equation (3), at steps of 0.02 h^{-1} within the interval $0 < n < 1$ h^{-1} (50 steps).

Table 3. Deposition velocity values at 50% relative humidity. Converted from cm s^{-1} in the original source [30].

Material	Ozone Deposition Velocity (v_d) [m h^{-1}]	Nitrogen Dioxide Deposition Velocity (v_d) [m h^{-1}]
Fine concrete	0.0612	0.0360
Brick	0.4320	0.2268
Wood-work surface treated	0.0198	0.0108
Metal	0.0050	0.0036
Synthetic floor covering	0.0202	0.0108

4.2. IAP Model

The concentration of organic acids was calculated by Equation (4) for the storage hall in three general scenarios:

- Sparsely filled with museum objects (as today) at a loading (L) of 0.7 m^2 m^{-3}
- Half-filled storage at L = 1.5 m^2 m^{-3}
- Full storage at L = 3 m^2 $m^{-3.}$

Only emission from wood was taken into account. The emission of organic acids directly affects the concentration in the air. As the emission rate is influenced by temperature (the higher temperature, the higher the emission rate) [10,56,57], the IAP modeling was carried out for the two extremes, a high summer and a low winter storage temperature. The model input is given in Table 4.

Table 4. Area-specific emission rate of wood (general), loading of objects, air exchange rate, and surface removal rate for the storage hall. *SER* data from [32].

Scenario	*SER* Winter [μg m^{-2} h^{-1}]	*SER* Summer [μg m^{-2} h^{-1}]	L [m^2 m^{-3}]	n [h^{-1}]	S [h^{-1}]
Sparsely filled storage (today)	50	200	0.7	0.02	2
Half full storage	50	200	1.5	0.02	2
Full storage	50	200	3	0.02	2
Full storage with filter recirculation	50	200	3	0.30 *	2

* Air exchange and filter removal combined.

Following this, it was modeled for each scenario how the organic acid concentration varied with a change in the air exchange rate (by ventilation or internal filtration). Calcu-

lations were performed in Microsoft Excel by Equation (4) at steps of 0.02 h^{-1} within the interval $0 < n < 10\ h^{-1}$ (500 steps).

4.3. Monte Carlo Simulation

A Monte Carlo simulation was used to model the indoor air pollution level following Equation (4). The simulation modeled the concentration based on the probability within a defined range for each of the four parameters. For simplicity, a uniform probability distribution was assigned between the minimum and maximum value of each variable of the pollution mass-balance. It may be that some factors are distributed differently (e.g., air exchange rate). However, more data are needed in order to verify this. The four parameters were considered independent.

The simulation was made by 1000 repetitions of Equation (4) where the value of each input parameter was selected randomly with a linear probability distribution using the SLUMP function (random number generator) in Microsoft Excel. The input data for the area-specific emission rate (*SER*) from wood were taken from a study on the emission from three heritage wood object samples [10] in winter and summer temperature conditions. Qualified estimates of possible ranges of *L*, *n*, and *S* were based on previous model studies [31,32]. Model input conditions (parameter intervals) are given in Table 5.

Table 5. Monte Carlo simulation input data. *SER* ranges from [10]. Intervals of *L*, *n*, and *S* were estimated based on [31,32].

Input Factor	Interval
SER, winter [μg m^{-2} h^{-1}]	39–108
SER, summer [μg m^{-2} h^{-1}]	145–303
L, low: Sparsely filled storage [m^2 m^{-3}]	0.4–0.9
L, high: Full storage [m^2 m^{-3}]	3–5
n [h^{-1}]	0.01–1
S [h^{-1}]	0.2–2

As the organic acid emission from heritage collections depends on temperature, one simulation was made for winter and one for a summer scenario. Furthermore, a simulation was first conducted for the present conditions (sparsely filled storage), and then repeated for a filled storage room. Thus, four scenarios were simulated:

A. Storage hall as now, sparsely loaded with objects, winter temperature.
B. Storage hall as now, sparsely loaded with objects, summer temperature.
C. Storage hall at full capacity, filled with objects, winter temperature.
D. Storage hall at full capacity, filled with objects, summer temperature.

A reservation must be made: Data for temperature-dependent emission rates are scarce, and it has not been possible to find input values for the exact temperature range in the hall. Our summer input relates to tests conducted at a standard room test temperature of 23 °C. It is, therefore, possible that the summer conditions will be overestimated, and the resulting summer concentration must therefore be considered an absolute worst-case scenario.

4.4. Pollution Measurements at Site

The concentration of ozone, nitrogen dioxide, and organic acids (acetic acid and formic acid) were measured shortly after the storage facility was taken into use. Sampling was conducted by the use of passive samplers (badge type) supplied and analyzed by The Swedish Environmental Research Institute IVL (Gothenburg, Sweden, www.ivl.se (accessed on 1 May 2023)). Sampling was carried out in duplicates for an exposure period of one month. Indoor samplers were mounted with metal clips on a shelf-end, half-ways between the floor and the ceiling. Outdoor samplers were mounted at 2 m height under a rain screen on a pole placed on an open grass lawn. Conditions were not yet representative of normal storage operation (empty storage hall, start-up adjustment of the ventilation

system, increased traffic through docking gate, etc.), but can be regarded as background screening. Follow-up measurements will be made in the coming years as the storage is gradually being filled.

5. Results

5.1. I/O Model Results

For a constant air exchange rate of 0.02 h^{-1} and a fully loaded storage room (Table 2) the I/O ratio was for ozone 0.19 and for nitrogen dioxide 0.29. If all collection objects were removed from the model (bare room with only concrete walls, ceiling, and floor) the I/O ratio increased to 0.37 for ozone and 0.50 for nitrogen dioxide. The fate of pollutants which enter the storage is shown in Figure 4, where the distribution of the materials the pollutants deposit onto are shown, together with the fraction leaving the room again via the air exchange. For ozone, 53% will deposit on the heritage objects (wood), while for nitrogen dioxide, only 14% ends up onto the collection. The rest is lost on building surfaces or removed again by ventilation.

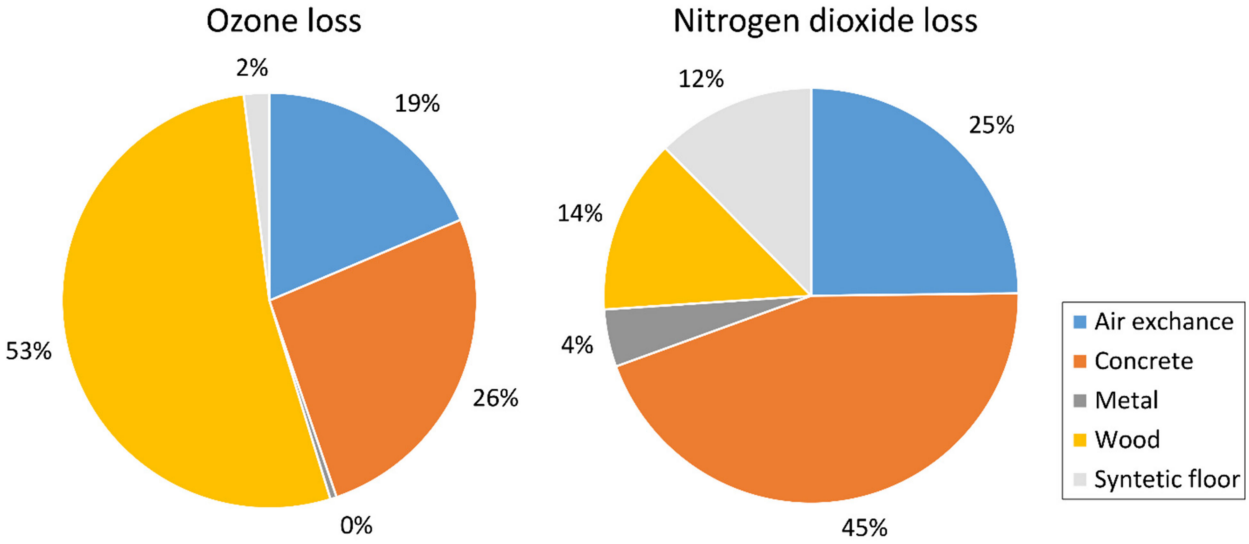

Figure 4. The fate of ozone and nitrogen dioxide in a full storage room (28,000 m^2 of wooden objects). The charts show the percentage distribution between sorption on different materials and removal by ventilation.

As the I/O ratio strongly depends on the air exchange rate, it is shown in Figure 5 how the I/O ratio for ozone and nitrogen dioxide will increase if the ventilation rate increases, and vice versa. This is illustrated for air changes up to 1 h^{-1}. The surface removal rates for the storage room, as calculated on the basis of Tables 2 and 3, were rather low, for ozone 0.1, and for nitrogen dioxide 0.05 h^{-1}. As an imaginary example of an indoor environment with a higher surface removal rate, Figure 5 also shows the I/O ratio for a room with S = 3 h^{-1}, which is a mid-range condition for typical occupied buildings such as homes, shops, offices, and museum exhibitions, having a variety of highly sorptive surfaces, such as carpets and furniture textiles [24].

5.2. IAP Model Results

The span in organic acid concentrations between summer and winter conditions is shown in Figure 6, assuming an air exchange rate of 0.02 h^{-1} (1/2 room volume per day) for the situation of the storage hall today (sparsely filled), and as it will gradually become filled up (input data from Table 4). For the full storage, the effect of adding the current filtration system (0.3 h^{-1} clean air delivery rate) was also tested.

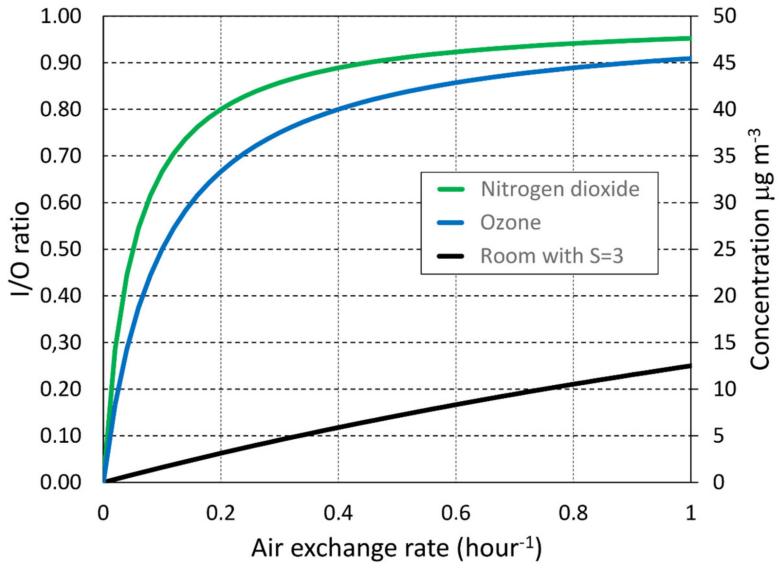

Figure 5. The I/O ratio of ozone and nitrogen dioxide in the storage hall when full as a function of the air exchange rate. Also shown is a room with a surface removal rate $S = 3\ h^{-1}$.

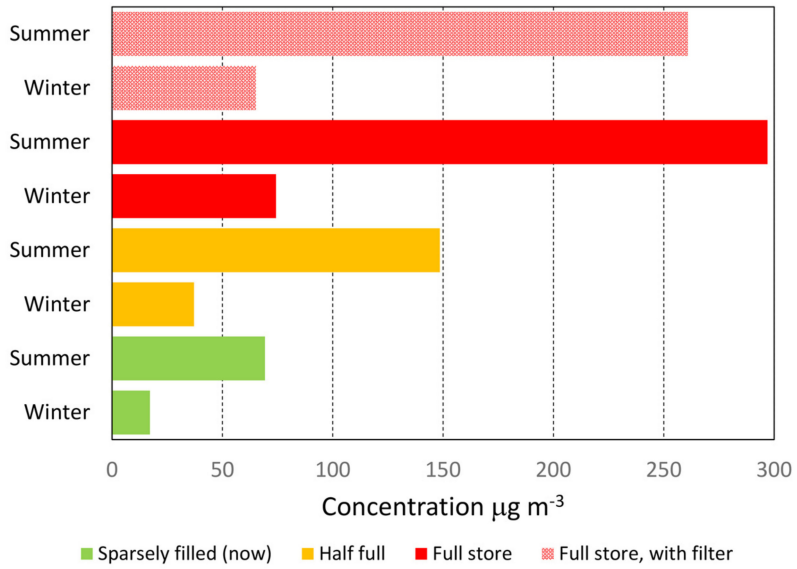

Figure 6. Organic acid concentration at winter and summer temperature inside the storage hall at different degrees of loading with wooden objects. At the top, in red, is shown the full storage with and without air filtration turned on.

In Figure 7 it is shown how the steady-state concentration of organic acids changes if the air exchange rate varies. This is illustrated for air changes up to $10\ h^{-1}$, which covers a range from solely naturally ventilated buildings up to a high rate of forced ventilation (with new air and/or by internal filtration). The models are shown for winter and summer temperature, and at each instance for the three general scenarios: Sparsely filled with wooden museum objects (as today) at a loading (L) of 0.7 $m^2\ m^{-3}$, a half-filled storage room at $L = 1.5\ m^2\ m^{-3}$; and a full storage at $L = 3\ m^2\ m^{-3}$.

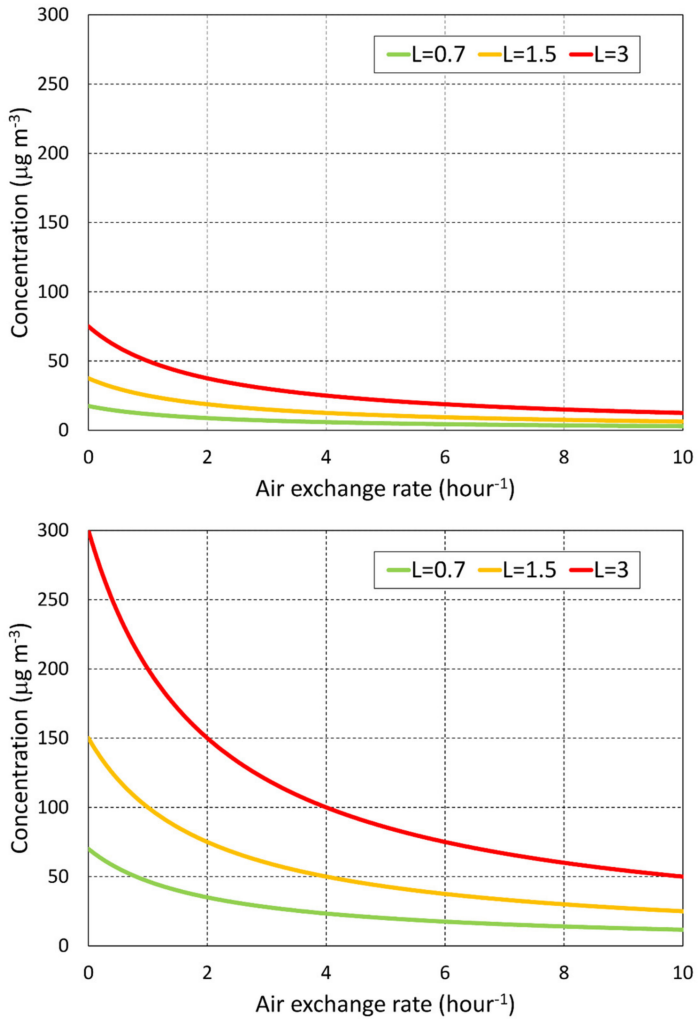

Figure 7. The concentration of organic acids as a function of the air exchange rate at winter temperature (**top**) and at summer temperature (**bottom**). For each scenario: Full room (L = 3 m^2 m^{-3}), half-full room (L = 1.5 m^2 m^{-3}); sparsely filled room (L = 0.7 m^2 m^{-3}).

5.3. Monte Carlo Simulation Results

The distribution of probable organic acid concentrations is given in Figure 8 below. The output from each of the 1000-iterations model runs was collected into pillars of intervals of 50 µg m^{-3} in a probability density histogram (0–50, 51–100, 101–150, a.s.o.). The simulation output presents the likely span of the indoor air pollution level for: (A) Sparsely filled storage room in winter, (B) sparsely filled storage in summer, (C) full storage in winter, (D) full storage in summer. The sparsely filled storage reflects the status of the facility at the time of writing. For each simulation, the median, average, minimum, and maximum 95% confidence interval bounds are shown in Table 6.

Table 6. The minimum and maximum 95% confidence interval bounds, median and average concentration [µg m^{-3}] for each Monte Carlo simulation (1000 iterations).

Simulation	5th Percentile	Median	Average	95th Percentile
A	15.3	29.3	30.9	51.5
B	53.3	88.5	91.9	144
C	56.0	115	123	215
D	197	360	377	648

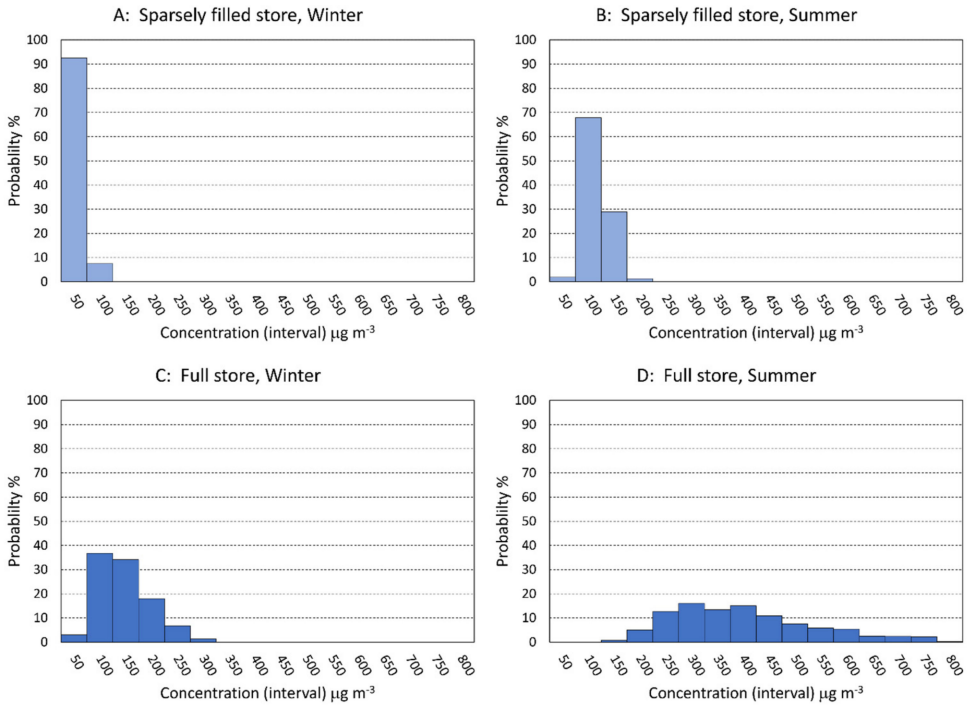

Figure 8. The probability distribution of pollution levels for the storage building as today (sparsely filled) in winter (**A**) and summer (**B**) conditions, and when filled with objects in winter (**C**) and summer (**D**) conditions.

In order to establish the least necessary number of simulation iterations, the result (average concentration) and the spread (standard deviation) of repeating a simulation ten times were compared for the modeling scenario C at 10, 100, 1000, and 2000 iterations. At 1000 and 2000 iterations, the results were very similar (average 123.4 and 122.7, both with a standard deviation of 1), which indicated that 1000 iterations were enough to obtain stable and reliable results (Figure 9).

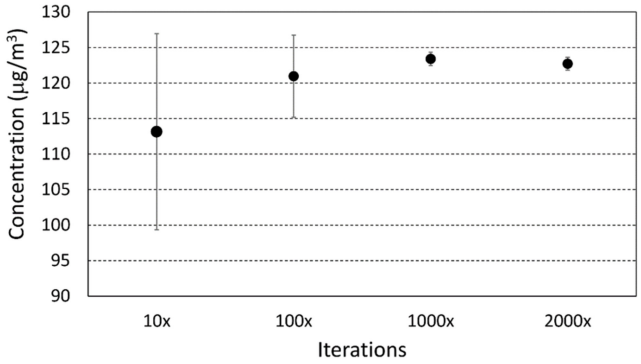

Figure 9. The average and standard deviation of 10 repeated simulations of scenario C at 10, 100, 1000, and 2000 iterations.

5.4. Pollution Measurements

The measured concentrations are reported in Table 7. Each value is the average of a duplicate measurement. Organic acids were only measured indoors.

Table 7. Passive sampling results for air pollutants indoors and outdoors. The indoor-to-outdoor ratio is given for ozone and nitrogen dioxide.

Location	Ozone	Nitrogen Dioxide	Organic Acids
Indoor concentration [μg m^{-3}]	1	0.2	12
Outdoor concentration [μg m^{-3}]	52	5.1	n.a.
I/O ratio [dimensionless]	0.02	0.04	n.a.

6. Discussion and Conclusions

6.1. Background Measurements

The pollution measurements by passive sampling, which were performed at the beginning of the operation of the building, revealed a low concentration of organic acids indoors (12 μg m^{-3}), and a low ingress of outdoor pollutants (I/O ratio = 0.02–0.04) (Table 7). The I/O model. However, predicted higher ratios for ozone 0.19, and for nitrogen dioxide 0.29, even had the storage room been full of objects. On the other hand, the low organic acid concentration reflects well a storage almost without wooden objects.

6.2. Outdoor Pollutants

While we acknowledge that the initial pollution measurement was done at a time when normal operation routines within the building had not yet come fully into force, the difference in outdoor pollutants between real measurements and the model calls for a closer examination. As displayed in Figure 5, the I/O ratio is highly influenced by air change. Although the air exchange rate of the hall is unknown, it is unlikely that it was much lower than our estimate of 0.02 h^{-1}. A more likely explanation is that the single-zone model has limitations if real buildings have a more complicated geometry than just one room. Perhaps the ingress of air had a more tortuous path into the storage hall than just through the nearest doors so that adjacent rooms became secondary zones between the storage area and ambient air. In that case, the indoor pollution level would become a fraction of the levels in the adjacent zones, which were a fraction of ambient, etc. However, in order to investigate such behavior in detail, air exchange measurements using several tracer gases at the same time are required [57], and the ignored influence of internal airflow between adjacent areas is a general weakness of single-zone models.

Another plausible explanation for the low I/O ratio is the additional effect of air filtration. Assuming filtration was on full-time, the current filtration system would deliver 0.3 room volumes of clean air per hour. This can be added to Equation (3) as a contributing loss (Q):

$$\frac{C_i}{C_o} = \frac{n}{n + (S_1 + S_2 + S_3 + \ldots) + Q_{filter}} \quad (5)$$

(input parameters: n = 0.02; $S_{total\text{-}ozone}$ = 0.1; $S_{total\text{-}NO2}$ = 0.05; Q_{filter} = 0.3).

Which, in that case, lowers the I/O ratio to 0.05 for both ozone and nitrogen dioxide, a level close to the real-life measurements.

An important feature of the I/O model is the illustration of the distribution of pollution loss. The collection received 53% of the indoor ozone and 14% of the nitrogen dioxide. Had the collection contained larger fractions of sorptive materials, such as textiles, this would have received an even higher part of the pollution deposition. This clarifies a dilemma, which is that storing many collection items will help clean the air. However, it will happen at the cost of the harmful pollutants' deposition onto the collection. Deliberate exploitation of exposing large surface areas is indeed an efficient pollution control strategy, as long as the sacrificial material is something other than the collection, e.g., sorptive wall covering [58]. In the planning of such actions, the I/O model will be a useful tool for estimating the effect of applying pollution-scavenging materials in rooms.

As previously mentioned, another shortcoming of the I/O model is the ignoring of atmospheric reactions. Studies in museum buildings have demonstrated how ozone and nitrogen oxide may react indoors and produce nitrogen dioxide beyond what is already introduced by ventilation, sometimes to a level of I/O > 1 [29]. In an American museum gallery, three weeks of measurements showed a loss distribution for ozone where surface uptake accounted for 62%, reactions with nitrogen oxide 31%, nitrogen dioxide 2%, and sorption on occupants for 5% [43]. In other words, for a model, which only accounts for surface and air exchange removal, the result may be underestimated by 30–40%, and this must be taken into account, especially for situations with a high influx of outdoor pollutants (high air exchange rate).

6.3. Indoor-Generated Pollutants

The IAP model, as run either as a single calculation based on fixed conditions or by the Monte Carlo simulation based on plausible intervals of each factor, offered a fair estimate of how the indoor pollution level will react to the continuous filling up of the storage area with wooden objects. For the storage still only sparsely filled (L = 0.7 m^2 m^{-3}), the most probable concentration levels were within well-defined intervals (0–50 in winter and 50–100 µg m^{-3} in summer). For a full storage room (L = 3 m^2 m^{-3}), the spread of the most probable concentration range was much wider, especially in summer (between about 200–500 µg m^{-3}), due to the wider summer intervals of the decisive factor *SER*.

In general, the difficulties in measuring L and n, as well as the little data available on *SER*, add uncertainty to the model. Besides scarce *SER* values for heritage materials as such, data are lacking the actual temperature interval of the storage facility. We used data measured at 10–23 °C, as this is what was available in the literature. However, the storage hall is intended to be cooler (at least below 20 °C), although this has not yet been verified by a full year of measurement. This winter (2022–2023), the lowest indoor temperature was 11 °C, and we still have to observe a summer period at normal operation. The uncertainty of the temperature level may, therefore, lead to an overestimation of the concentration level in summer. In any case, the model predicts how the organic acid level varies between the seasons, and while we still need to test the exact values by measurement when normal operation has been set up, the trend has been laid out. Previous monitoring in another storage building of The National Museum convincingly illustrated the same behavior [57], which we, based on the modeling, also expect to observe in the new storage hall (Figure 10).

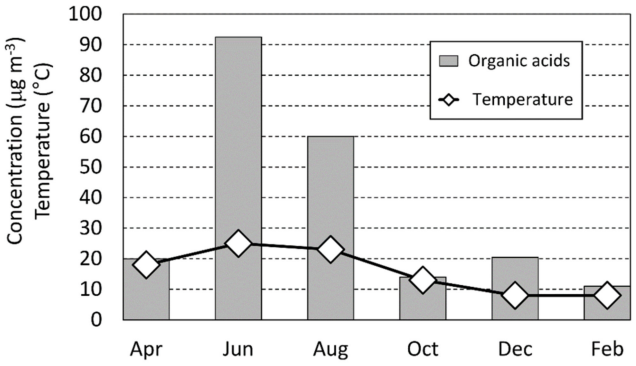

Figure 10. Organic acid concentration and temperature during one year in the storage room of the National Museums of Denmark's Music Museum. Data from [57] (converted from ppb).

6.4. Constant versus Dynamic Conditions

The static nature of steady-state models is a challenge when applied to dynamic environments. Although we assume a number of factors to be constant, they may, as discussed in the introduction, in fact, be of a dynamic nature (Figure 1). Examples are the emission rate, which may vary with the annual seasons due to the influence of temperature, or the air exchange rate, which may vary due to changes in weather and peoples' use of the building. The dynamic nature of an indoor environment can be demonstrated by a

continuous series of instant ozone measurements performed at yet another of the National Museum's storage buildings (Figure 11). When measured at a resolution of 1-h intervals, it was revealed how the indoor level varied sometimes more than 10 μg m^{-3} per day, in a pattern closely following the outdoor ozone level. Over the twelve days shown in Figure 11, the average I/O ratio was 0.39. However, on a short-term basis, it cycled between 0.25 and 0.70. This would rarely be reflected in a steady-state simple I/O modeling, as the input values often are long-term average values (e.g., passive sampling measurements carried out over periods of weeks or longer).

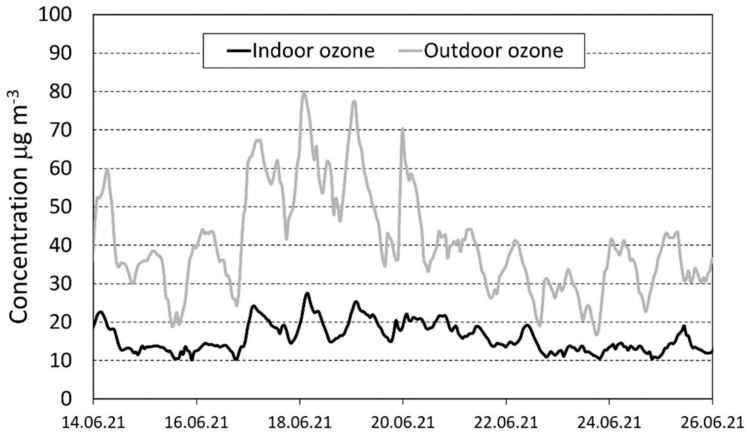

Figure 11. Twelve days of continuous ozone measurements inside and outside The National Museum of Denmark's storage facility Ørholm (unpublished data by the authors).

Although Monte Carlo simulations reflect the possible outcomes at steady-state conditions, the spread of results also reflects the possible numerical extent of the short dynamic variations (however, not necessarily distributed in the same way). Real dynamic condition modeling would require a large amount of data, and all factors should be available in time-resolved high resolution in order to show their mutual influence on the concentration over time. However, as argued previously, for conservation risk management, this is an unnecessary level of detail when long-time average concentration is sufficient for dose calculations for the assessment of materials damage risks.

6.5. Practical Implications and Perspectives

For our example, the National Museum's storage hall in Vinge, modeling showed that outdoor pollutants are efficiently retarded by the low air exchange of the building. Furthermore, the additional air filtration rate of 0.3 h^{-1} provides sufficient control. The indoor generated organic acids may be expected in a level up to about 300 (plausible range 200–500) μg m^{-3} in summer, once the storage hall has been filled with objects. However, should summer temperature turn out to be much lower than 20 °C, the concentration will be correspondingly smaller as well. Wintertime levels are expected to be less than 100 μg m^{-3}.

If desired, the organic acid concentration can be decreased by filtration. However, for the indoor generated pollutants, the flow rate of the current filtration system is inadequate. According to Figure 7, the filter recirculation rate (clean air delivery rate) should be 2 h^{-1} to halve the level at current conditions or 4 h^{-1} to lower it to one-third. In any case, a decision to increase filtration should be based on assessing the potential risk for the actual collection and the question of whether there are particularly susceptible objects present. Even for the least probable high concentrations predicted by the Monte Carlo simulation, the level is below the maximum average level of 1000 μg m^{-3} recommended by ASHRAE for a general museum collection [16].

As the museum storage hall is still just beginning to be filled up, it will take some time before true steady-state conditions enter into force. Our planned follow-up monitoring of the pollution levels over the coming years will reveal how well the models actually

predicted the reality. More data are needed in order to improve input for the models. The authors encourage readers to share data from pollution monitoring in heritage buildings, as well as any experiences in using the I/O and IAP models, in order to refine them and validate their use.

The models presented here are practical for assessing the impact of indoor and outdoor pollution loads in a building. Even for fast and overall screening, it will be easy to establish the order of magnitude estimates, from which it can be decided whether a problem needs to be addressed in more detail. In our example, the modeling revealed a need to investigate further the air exchange between adjacent indoor areas, and to establish the overall air exchange rate. Steady-state models allow, with a minimum of input data, to assess indoor conditions based on basic properties or as the result of initiated control actions (e.g., increased ventilation, applying filters, etc.), and by this contribute as a tool for better practice in air quality management in heritage buildings.

Author Contributions: Conceptualization, methodology, formal analysis, investigation, software, data curation, writing—review and editing, M.R.-S. and S.H.S.; writing—original draft preparation, M.R.-S. All authors have read and agreed to the published version of the manuscript.

Funding: This research received no external funding.

Data Availability Statement: The model input data are available in tables in the article.

Acknowledgments: We thank the management of the National Museum of Denmark for permission to use the storage buildings as the subject of our research. We especially thank conservator Lars Aasbjerg Jensen, National Museum of Denmark, for providing information and data about the building, and for practical support during site visits.

Conflicts of Interest: The authors declare no conflict of interest.

References

1. Baer, N.S.; Banks, P.N. Indoor air pollution: Effects on cultural and historic materials. *Int. J. Mus. Manag. Curatorship* **1985**, *4*, 9–20.
2. Brimblecombe, P. The composition of museum atmospheres. *Atmos. Environ. Part B Urban Atmos.* **1990**, *24B*, 1–8. [CrossRef]
3. Graedel, T.E.; McGill, R. Degradation of materials in the atmosphere. *Environ. Sci. Technol.* **1986**, *20*, 1093–1100. [CrossRef]
4. Blades, N.; Oreszczyn, T.; Bordass, B.; Cassar, M. *Guidelines on Pollution Control in Museum Buildings*; Museums Association: London, UK, 2000.
5. Hatchfield, P. *Pollutants in the Museum Environment-Practical Strategies for Problem Solving in Design, Exhibition and Storage*; Archetype Publications Ltd.: London, UK, 2002.
6. Tétreault, J. *Airborne Pollutants in Museums, Galleries and Archives: Risk Assessment, Control Strategies and Preservation Management*; Canadian Conservation Institute: Ottawa, ON, Canada, 2003.
7. Paterakis, A.B. *Volatile Organic Compounds and the Conservation of Inorganic Materials*; Archetype Publications Ltd.: London, UK, 2016.
8. Gray, V.R. The Acidity of Wood. *J. Wood Sci.* **1958**, *1*, 58–64.
9. Clarke, S.G.; Longhurst, E.E. The Corrosion of Metals by Acid Vapours from Wood. *J. Appl. Chem.* **1961**, *11*, 435–443. [CrossRef]
10. Smedemark, S.H.; Ryhl-Svendsen, M.; Schieweck, A. Quantification of formic acid and acetic acid emissions from heritage collections under indoor room conditions. Part I: Laboratory and field measurements. *Herit. Sci.* **2020**, *8*, 58. [CrossRef]
11. Smedemark, S.H. The dynamics and control of indoor air pollution in repositories without mechanical ventilation for cultural heritage collections. A literature review. *e-Preservation Sci.* **2018**, *15*, 17–29.
12. Grzywacz, C.M. Using Passive Sampling Devices to Detect Pollutants in Museum Environments. In *ICOM Committee for Conservation, Proceedings of the 10th Triennial Meeting, Washington, DC, USA, 22–27 August 1993*; Bridgland, J., Ed.; James & James: London, UK, 1993; pp. 610–615.
13. Ryhl-Svendsen, M.; Smedemark, S.H. Environmental conditions for Danish storage buildings: Reviewing 20 years of air quality surveys. *Stud. Conserv.* **2023**. (*submitted*).
14. Ryhl-Svendsen, M. Indoor air pollution in museums: Prediction models and control strategies. *Stud. Conserv.* **2006**, *51* (Suppl. S1), 27–41. [CrossRef]
15. Dabanlis, G.; Loupa, G.; Tsalidis, G.A.; Kostenidou, E.; Rapsomanikis, S. The Interplay between Air Quality and Energy Efficiency in Museums, a Review. *Appl. Sci.* **2023**, *13*, 5535. [CrossRef]
16. ASHRAE. Museums, Galleries, Archives, and Libraries. In *ASHRAE Handbook-HVAC Applications*; American Society of Heating, Refrigerating and Air-Conditioning Engineers: Atlanta, GA, USA, 2019; Chapter 24.
17. Grzywacz, C.M. *Monitoring for Gaseous Pollutants in Museum Environments*; (Tools for Conservation); The Getty Conservation Institute: Los Angeles, CA, USA, 2006.

18. Brimblecombe, P. The balance of environmental factors attacking artifacts. In *Durability and Change. The Science, Responsibility, and Cost of Sustaining Cultural Heritage. Dahlem Workshop, Berlin, Germany, 1992*; Krumbein, W.E., Brimblecombe, P., Cosgrove, D.E., Staniforth, S., Eds.; John Wiley & Sons: New York, NY, USA, 1994; pp. 67–79.
19. Brimblecombe, P. Pollution Studies. In *ENVIRONMENT Leather Project Deterioration and Conservation of Vegetable Tanned Leather*; Larsen, R., Ed.; Protection and Conservation of the European Cultural Heritage, Research Report No. 6 of European Commission; The Royal Danish Academy of Fine Arts: Copenhagen, Denmark, 1996; pp. 25–32.
20. Abdalla, T.E.; Peng, C. Evaluation of housing stock indoor air quality models: A review of data requirements and model performance. *J. Build. Eng.* **2021**, *43*, 102846. [CrossRef]
21. Pepper, D.W.; Carrington, D. *Modeling Indoor Air Pollution*; Imperial College Press: London, UK, 2009.
22. Weschler, C.J.; Shields, H.C.; Naik, D.V. Indoor Ozone Exposures. *J. Air Pollut. Control. Assoc.* **1989**, *39*, 1562–1568. [CrossRef]
23. Nazaroff, W.W.; Gadgil, A.J.; Weschler, C.J. Critique of the use of deposition velocity in modeling air quality and exposure. In *ASTM Special Technical Publication: Modeling of Indoor Air Quality and Exposure*; Nagda, N.L., Ed.; ASTM STP 1205; American Society for Testing and Materials: Philadelphia, PA, USA, 1993; pp. 81–104.
24. Weschler, C.J. Ozone in indoor environments: Concentration and chemistry. *Indoor Air* **2000**, *10*, 269–288. [CrossRef] [PubMed]
25. Blades, N.; Kruppa, D.; Cassar, M. Development of a web-based software tool for predicting the occurrence and effect of air pollutants inside museum buildings. In *ICOM Committee for Conservation, Proceedings of the 13th Triennial Meeting, Rio de Janeiro, Brazil, 22–27 September 2002*; Verger, I., Ed.; James & Jamens: London, UK, 2002; pp. 9–14.
26. Spicer, C.W.; Kenny, D.V.; Ward, G.F.; Billick, I.H. Transformations, Lifetimes, and Sources of NO_2, HONO, and HNO_3 in Indoor Environments. *J. Air Waste Manag. Assoc.* **1993**, *43*, 1479–1485. [CrossRef]
27. Febo, A.; Perrino, C. Prediction and experimental evidence for high air concentration of nitrous acid in indoor environments. *Atmos. Environ.* **1991**, *25A*, 1055–1061. [CrossRef]
28. Katsanos, N.A.; De Santis, F.; Cordoba, A.; Roubani-Kalantzopoulou, F.; Pasella, D. Corrosive effects from the deposition of gaseous pollutants on surfaces of cultural and artistic value inside museums. *J. Hazard. Mater. A* **1999**, *64*, 21–36. [CrossRef] [PubMed]
29. Brimblecombe, P.; Blades, N.; Camuffo, D.; Sturaro, G.; Valentino, A.; Gysels, K.; Van Grieken, R.; Busse, H.-J.; Kim, O.; Wieser, M. The indoor environment of a modern museum building, The Sainsbury Centre for Visual Arts, Norwich, UK. *Indoor Air* **1999**, *9*, 146–164. [CrossRef]
30. Grøntoft, T.; Raychaudhuri, M.R. Compilation of tables of surface deposition velocities for O_3, NO_2 and SO_2 to a range of indoor surfaces. *Atmos. Environ.* **2004**, *38*, 533–544. [CrossRef]
31. Ryhl-Svendsen, M. The role of air exchange rate and surface reaction rates on the air quality in museum storage buildings. In *Museum Microclimates, Proceedings of the Copenhagen Conference, Copenhagen, Denmark, 19–23 November 2007*; Padfield, T., Borchersen, K., Eds.; National Museum of Denmark: Copenhagen, Denmark, 2007; pp. 221–226.
32. Smedemark, S.H.; Ryhl-Svendsen, M. Determining the level of organic acid air pollution in museum storage rooms by mass-balance modelling. *J. Cult. Herit.* **2022**, *55*, 309–317. [CrossRef]
33. McVoy, G.R. Monte Carlo Simulation Techniques Applied to Air Quality Impact Assessment. *J. Air Pollut. Control Assoc.* **1979**, *29*, 843–845. [CrossRef]
34. Johnson, M.; Lam, N.; Brant, S.; Charron, D.; Gray, C.; Pennise, D. Modeling indoor air pollution from cookstove emissions in developing countries using a Monte Carlo single-box model. *Atmos. Environ.* **2011**, *45*, 3237–3243. [CrossRef]
35. Kruza, M.; Shaw, D.; Shaw, J.; Carslaw, N. Towards improved models for indoor air chemistry: A Monte Carlo simulation study. *Atmos. Environ.* **2021**, *262*, 118625. [CrossRef]
36. Dai, X.; Liu, J.; Zhang, X. Monte Carlo simulation to control indoor pollutants from indoor and outdoor sources for residential buildings in Tianjin, China. *Build. Eviron.* **2019**, *165*, 106376. [CrossRef]
37. Weschler, C.J.; Shields, H.C.; Naik, D.V. Indoor chemistry involving O_3, NO, and NO_2 as evidence by 14 months of measurements at a site in Southern California. *Environ. Sci. Technol.* **1994**, *28*, 2120–2132. [CrossRef] [PubMed]
38. Weschler, C.J.; Shields, H.C. Potential reactions among indoor pollutants. *Atmos. Environ.* **1997**, *31*, 3487–3495. [CrossRef]
39. Nazaroff, W.W.; Cass, G.R. Mathematical modeling of chemically reactive pollutants in indoor air. *Environ. Sci. Technol.* **1986**, *20*, 924–934. [CrossRef]
40. Carslaw, N. A new detailed chemical model for indoor air pollution. *Atmos. Environ.* **2007**, *41*, 1164–1179. [CrossRef]
41. Druzic, J.; Adams, M.; Tiller, C.; Cass, G.R. The measurement and model predictions of indoor ozone concentrations in museums. *Atmos. Environ.* **1990**, *24A*, 1813–1823. [CrossRef]
42. Drakou, G.; Zerefos, C.; Ziomas, I.; Gantis, V. Numerical simulation of indoor air pollution levels in a church and in a museum in Greece. *Stud. Conserv.* **2000**, *45*, 85–94.
43. Pagonis, D.; Price, D.J.; Algrim, L.B.; Day, D.A.; Handschy, A.V.; Stark, H.; Miller, S.L.; de Gouw, J.; Jimenez, J.L.; Ziemann, P.J. Time-resolved measurements of indoor chemical emissions, deposition, and reactions in a university art museum. *Environ. Sci. Technol.* **2019**, *53*, 4794–4802. [CrossRef]
44. Li, Y.; Nielsen, P.V. CFD and ventilation research. *Indoor Air* **2011**, *21*, 442–453. [CrossRef] [PubMed]
45. Grau-Bové, J.; Mazzei, L.; Strlic, M.; Cassar, M. Fluid simulations in heritage science. *Herit. Sci.* **2019**, *7*, 16. [CrossRef]
46. Ascione, F.; Bellia, L.; Capozzoli, A. A coupled numerical approach on museum air conditioning: Energy and fluid-dynamic analysis. *Appl. Energy* **2013**, *103*, 416–427. [CrossRef]

47. Grau-Bové, J.; Strlič, M. Fine particulate matter in indoor cultural heritage: A literature review. *Herit. Sci.* **2013**, *1*, 8. [CrossRef]
48. Mašková, L.; Smolík, J.; Ondráček, J.; Ondráčková, L.; Travnickova, T.; Havlica, J. Air quality in archives housed in historic buildings: Assessment of concentration of indoor particles of outdoor origin. *Build. Eviron.* **2020**, *180*, 107024. [CrossRef]
49. Grau-Bové, J.; Mazzei, L.; Malki-Ephstein, L.; Thickett, D.; Strlič, M. Simulation of particulate matter ingress, dispersion and deposition in a historical building. *J. Cult. Herit.* **2016**, *18*, 199–208. [CrossRef]
50. Camuffo, D. *Microclimate for Cultural Heritage: Measurements, Risk Assessment, Conservation, Restoration, and Maintaince of Indoor and Outdoor Monuments*, 3rd ed.; Elsevier: Amsterdam, The Netherlands, 2019; pp. 197–234.
51. Morawska, L.; Salthammer, T. Fundamentals. In *Indoor Environment, Airborne Particles and Settled Dust*; Morawska, L., Salthammer, T., Eds.; Wiley-WCH Verlag GmbH & Co. KGaA: Weinheim, Germany, 2003; pp. 1–46.
52. Fællesmagasinet (In Danish: The Joint Storage Facility). Danish Agency for Culture and Palaces. Available online: https://slks.dk/omraader/slotte-og-ejendomme/bygge-og-udviklingsprojekter/faellesmagasinet (accessed on 1 May 2023).
53. Janssen, H.; Christensen, J.E. Hygrothermal optimisation of museum storage spaces. *Energy Build.* **2013**, *56*, 169–178. [CrossRef]
54. Ryhl-Svendsen, M.; Jensen, L.A.; Larsen, P.K.; Bøhm, B.; Padfield, T. Ultra-low-energy museum storage. In *Proceedings of the ICOM-CC 16th Triennial Conference, Lisbon, Portugal, 19–23 September 2011*; Bridgland, J., Ed.; ICOM Committee for Conservation: Paris, France, 2011; p. 8.
55. Department of Environmental Sciences, Aarhus University. Air Quality Data. Available online: https://envs.au.dk/en/research-areas/air-pollution-emissions-and-effects/air-quality-data (accessed on 1 May 2023).
56. Smedemark, S.H.; Ryhl-Svendsen, M. Indoor air pollution in archives: Temperature dependent emission of formic acid and acetic acid from paper. *J. Pap. Conserv.* **2020**, *21*, 22–30. [CrossRef]
57. Ryhl-Svendsen, M.; Jensen, L.A.; Larsen, P.K. Air quality in low-ventilated museum storage buildings. In *ICOM Committee for Conservation, Proceedings of the 17th Triennial Conference Preprints, Melbourne, Australia, 15–19 September 2014*; Bridgland, J., Ed.; International Council of Museums: Paris, France, 2014; p. 8.
58. Ryhl-Svendsen, M.; Clausen, G. The effect of ventilation, filtration and passive sorption on indoor air quality in museum storage rooms. *Stud. Conserv.* **2009**, *54*, 35–48. [CrossRef]